RESEARCH ARTICLE OPEN ACCESS

Formation and Morphology of Architectural Surfaces Design

Arthur Perez Rivao[1], Lisbeth A. Brandt-Garcia[2*], Rocio R. Gallegos-Villela[2], Josue F. Perez-Sanchez[3].

[1] Facultad de Química. Universidad de la Habana, Cuba.

[2]Facultad de Arquitectura, Diseño y Urbanismo. Universidad Autónoma de Tamaulipas. México.

[3]ITCM. Ciudad Madero, Tamaulipas. México.

*Corresponding author: lbrandt@docentes.uat.edu.mx

----------**********----------

Abstract:

Roughness is a characteristic property of solid surfaces, and its modification by physical and chemical treatments is of great importance when certain uses of materials are required on an industrial or laboratory scale. Properties such as adsorption, heat transmission, and the efficiency of a catalyst depend largely on surface roughness. At present, a better surface finish is increasingly necessary to optimize the use of certain products. A very complicated surface finish becomes a higher cost and production time, hence the importance of knowing how this property depends on the solid formation process. The present work is based on the hypothesis that the fractal dimension of the surface of a solid-solid dispersed system depends on the surface area and the composition of the particles that form the dispersed phase. From this hypothesis, it is established as a general objective to experimentally determine the relationship between the fractal dimension, the size of particles and the composition of a dispersed system formed by cement (dispersion medium) and stone dust (dispersed phase).

Keywords **—graphic analysis material, .**

----------**********----------

INTRODUCTION

The surface roughness constitutes a manifestation of the set of irregularities present on a solid surface [1,2] (Figure 1), and its quantification is possible by analyzing the fractal dimension of the plot of the profile of a given surface [3]. The profile of a surface is identified with the line obtained at the intersection between the surface and a plane perpendicular to it (Figure 2).

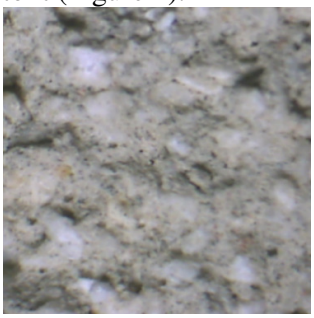

Figure 1. Microscopic image of a solid Surface

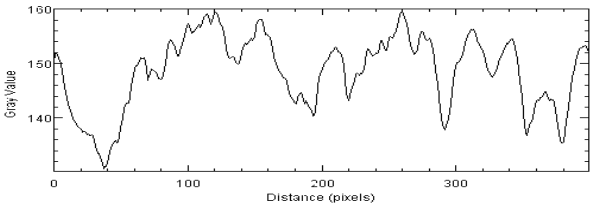

Figure 2 Plotting of the surface profile shown in Figure 1

The local roughness of a solid surface can be quantified through the Hurt coefficient or local roughness exponent [4], defined as:

$$H = 2 - f \quad (1)$$

With f being the fractal dimension of the surface profile, less rough surfaces will correspond to higher values of the fractal dimension.

The fractal dimension is an exponent that indicates how much a fractal can fill a space of n dimensions y may be applied to many areas as architecture and design [5]. This is determined through an image of the surface in an 8-bit format by the method of counting boxes (box counting), which consists of dividing the image into square cells of size l and counting the number of these in which There are elements of the fractal [6]. The size of the cells is progressively decreased, and the fractal dimension is calculated through the relationship:

$$f = \lim_{n-0} \frac{lnNo(l)}{lnNt} \quad (2)$$

Where No (l) is the number of cells of size l occupied by the fractal and Nt (l) is the number of total cells

The closer the length of the cells is closer to zero, the more accurate the result will be, however, there is a limit for this length, which in the case of images is the pixel, so a higher resolution result will be obtained from higher resolution images. Fewer mistakes The length of a line drawn on an irregular solid surface cannot be determined through Euclidean geometry, so to carry out this determination, fractal geometry is used, through the expression:

$$\boldsymbol{L_f = \delta^{1-f} \times L^f} \quad (3)$$

Where:
Lf: fractal length
δ: measurement coefficient
L: euclidean length
f: fractal dimensión

In the case of the surface area, using fractal geometry, it is expressed as:

$$\boldsymbol{A = \delta^{2-f_1-f_2} L^{f_1} \times L^{f_2}} \quad (4)$$

L1fractal and L2fractal being the lengths of two perpendicular lines drawn on the surface.

METHOD

To carry out the experimental procedure, a sieve was used to separate the dust particles into different average particle diameters, using those having an average diameter of 0.071, 0.2, 0.25 and 0.35 mm, respectively. The mixtures were prepared using typical construction materials; in this case, a mixture of powder and cement was used, varying the proportion of cement between 15 and 25% in dry mass. After the dried samples were prepared, they were mixed with water, and these were allowed to stand for 72 hours on slide sheets. During the resting process a chemical reaction of crystallization of the cement takes place resulting in the formation of a solid-solid dispersed system in which it is considered that the sand particles form the dispersed phase and the crystallized cement the dispersionmedium.

Photos of the surfaces of the solids were taken using a NOVEL brand microscope with X20 magnification and an HDCE-10 camera connected to a computer. The images were obtained with a format of 1024 × 768 pixels. The computational work of the edition of the images was carried out with the ImageJ version 1.51J8 program which can be downloaded for free from the page http://imagen.nih.gov/ij. Using the ImageJ program, the images were trimmed to a size of 400x400 pixels and converted to an 8-bit format. Once this was done, through the plot profile option, the plot of the sample profile was obtained and from this its fractal dimension. To determine the fractal dimension, the plotting of the profile is first necessary with the Analyze-Plot Profile options (Figure 3)

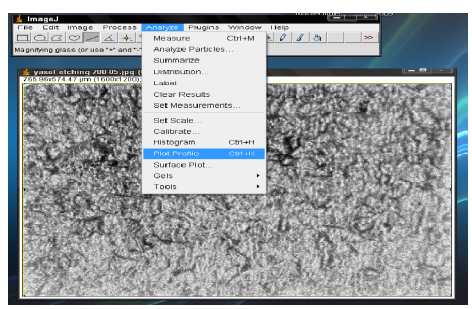

Figure 3. Option for surface plottingnce the profile plot is obtained, it becomes a binary image, and its fractaldimension is determined with the Process-Binary-Make Binare options (Figure 4), followed by the Analyze-Tools-Fractal Box Count options (Figure 5).

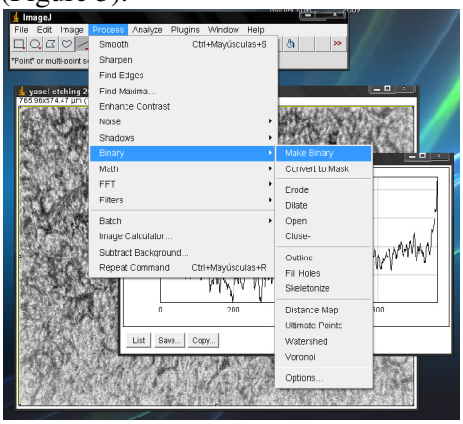

Figure 4. Option to convert the average pixel intensity profile into a binary image

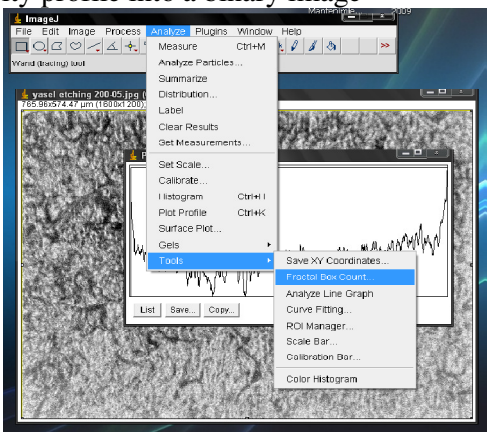

Figure 5. Option to calculate the fractal dimension of the profile

RESULTS AND DISCUSSION

The design of experiments was constituted by 12 experiments, with the fractal dimension (f) as a dependent variable, and with the surface area and the composition of the samples as independent variables with 4 and 3 levels. This design, as well as the results obtained after its execution, are shown in Table 1.

TABLE 1. RESULTS OF THE EXPERIMENTAL DESIGN

Sample	Surface area (mm2)	Composition (c)	Fractal dimension (f)
1	84,507	0,15	2,5561
2	30	0,15	2,538
3	24	0,15	2,5169
4	17,1428	0,15	2,4769
5	84,507	0,2	2,5842
6	30	0,2	2,5073
7	24	0,2	2,4835
8	17,1428	0,2	2,3477
9	84,507	0,25	2,5431
10	30	0,25	2,5011
11	24	0,25	2,4363
12	17,1428	0,25	2,4268

The experimental design analysis was carried out using the Statgraphics obtaining the following results:

Estimated effects for f

Estimated effects for f			
Effect	Dear	Error Dear	V.I.F
average	2.27181	0.0443188	
A:d	0.0193715	0.00473136	108.672
B:c	-0.0474321	0.026237	3.12175
AA	-0.00015426	4.4427E-05	108.672
AB	0.00064672	0.00055587	3.12175
BB	0.0395	0.0257203	1

Standard errors based on the total error with 6 g.l.

Analysis of variance for f					
Source	sc	Gl	CM	Reason -f	Value - P
A:d	0.00739291	1	0.00739291	16.76	0.0064
B:c	0.00144138	1	0.00144138	3.27	0.1206
AA	0.00531709	1	0.00531709	12.06	0.0133
AB	0.00059696	1	0.00059696	1.35	0.2888
BB	0.00104017	1	0.00104017	2.36	0.1755
Total error	0.00264614	6	0.00044102		

Total correct	0.0301047	11			

SC: Sum of squares
CM: Medium squares

R-square= 91,2102 percent
R-square (adjusted by g.l.) =83,8854 percent
Standard error of the estimate = 0,0210005
Average absolute error= 0,0130938
Statistician Durbin – Watson = 2,22493 (P=0,2402)
Residual autocorrelation of Lag 1=0,15571

specific surface area of the particles (mm2 / mm3), defined as the surface area divided by volume, calculated from considering the average particle size and that these are spherical. It is important to say that similar resulted can be obtained in other areas [7,8].

Figure 6 shows the Pareto chart that allows visualizing the effect of each of the independent variables considered on the fractal dimension. In this case it can be observed that the composition of the solid does not affect the value of the fractal dimension observed, at least for the composition intervals that were considered in this experiment, while the independent variable that does influence is the specific surface area, where The quadratic effect of this variable evidences a non-linear dependence between the fractal dimension and the specific surface area of the particle

The regression coefficient for f	
Coefficient	Dear
constant	2.68268
A:d	0.00839231
B:c	-3.63432
AA	-7.7131E-05
AB	0.0064672
BB	7.9

. Standardized Pareto Diagram for f

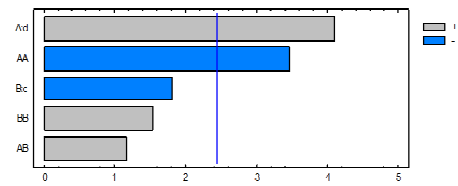

Standardized effect

Figure 6. Pareto diagram showing the effects of the independent variables A (specific surface area of the particles) and B (the composition of the dispersed system) on the fractal dimension. Based on the results observed and the analysis of the experimental design, the statistical adjustment of two models was carried out, one polynomial of degree 2 given by:

$$f = A + B \times a + Ca^2 \quad (5)$$

and another nonlinear given by:

$$f = \frac{H \times a + 2}{N \times a + 1} \quad (6)$$

where A, B, C, H, and N are determined by statistical techniques.
In the case of the non-linear model, the result was:

Estimation method: Marquardt
The estimate stopped due to convergence of the estimated parameters
Number of interactions: 8
Number of function calls: 25

Estimation results				95.00%
parameter	Dear	standard error Asymptotic	Asymptotic LOWER	HIGHER
H	0.400368	0.0744884	0.234397	0.566339
Q	0.153938	0.0299728	0.0871547	0.220722

Variance analysis			
Source	SC	Gl	CM
Model	74.4279	2	37.2139
Residue	0.00590349	10	0.00059035
Total	74.4338	12	
Total (Corr.)	0.0301047	11	

R- SQUARE=80,3902 PERCENT
R-SQUARE (ADJUSTED BY g.l.)=78,4292 percent

the standard error of est. =0,00242971
absolute mean error = 0,0177525
statistician Durbin – Watson = 1,59696
residual delay autocorrelation 1 = 0,183999

waste analysis

	Estimate	Validation
n	12	
CME	0.00059035	
MAE	0.0177525	
MAPE	0.719618	
ME	-5.5417E-05	
MPE	-0.0108977	

The fitted model is

$$f = \frac{0.400368 \times a + 2}{0.153938 \times a + 1}$$

THE FITTED MODEL IS

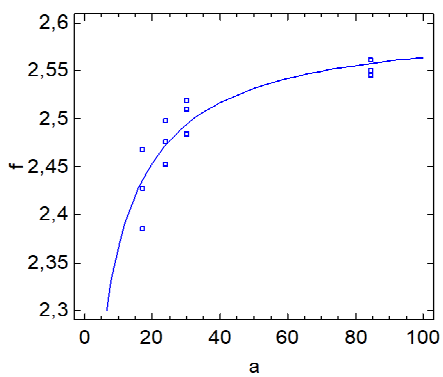

FIGURE 6. GRAPH OF THE FITTED MODEL

F GRAPH

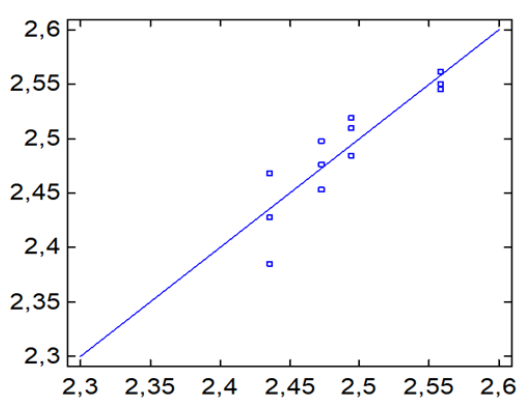

FORETOLD

Figure 7. Graph of observed vs. predicted behaviour

In the case of polynomial regression using the Stargraphics, the following was obtained.
Polynomial Regression - f versus a
Dependent variable: f
Independent variable: a
Order of the polynomial = 2

		Error	Estatistical	
Parameter	Dear	Standard	T	Value-P
constant	2,23402	0,0801459	27,8744	0,0000
a	0,0125193	0,00436082	2,87085	0,0185
a^2	-0,000102363	0,0000409588	-2,49916	0,0339

VARIANCE ANALYSIS

source	sum of pictures	Gl	middle square	Reason-F	Value-P
Modelo	0,0332517	2	0,0166259	11,10	0,0037
Residual	0,0134822	9	0,00149802		
Total (Corr.)	0,0467339	11			

R-square = 71,1511 percent
R-square (ajustada por g.l.) = 64,7403 percent
standard error of est. = 0,0387043
Average absolute error = 0,0265996
Statistical Durbin-Watson = 1,17482 (P=0,0845)
waste autocorrelation lag 1 = 0,409143

The StatAdvisor

The output shows the results of fitting a second order polynomial model to describe the relationship between f and a. The equation of the fitted model is

1) f = 2,23402 + 0,0125193*a-0,000102363*a^2

Since the P-value in the ANOVA table is less than 0.05, there is a statistically significant relationship between f and with a 95% confidence level.

The R-Square statistic indicates that the model thus adjusted explains 71.1511% of the variability in f. The adjusted R-Square statistic, which is more appropriate for comparing models with different numbers of independent variables, is 64.7403%. The standard error of the estimate shows that the standard deviation of the residues is 0.0387043.

This value can be used to construct limits for new observations by selecting the Reports option from the text menu. The mean absolute error (MAE) of 0.0265996 is the average value of the waste. The Durbin-Watson (DW) statistic examines the residuals to determine if there is any significant correlation based on the order in which they are presented in the data file. Since the P-value greater than 0.05, there is no indication of serial correlation in the residuals, with a 95% confidence level.

To determine if the order of the polynomial is appropriate, first note that the P-value in the highest order term is equal to 0.0339087. Since the P-value is less than 0.05, the higher order term is statistically significant, with a 95% confidence level. Consequently, it is likely that he would not want to consider any minor order model.

FITTED MODEL CHART

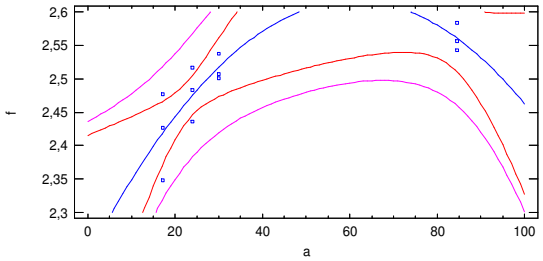

CONCLUSIONS

The analysis of the data using the STARGRAPHICS program showed that the fractal dimension depends to a greater extent on the diameter of the particles while the influence of the composition is negligible. In this paper analysis description is applied in a real material surface used in architectonic edification, but it is useful for other analysis in the graphic design, architecture, and material formal characterization among others. It was also observed that the roughest surfaces were those that had particles of smaller surface area.

REFERENCES

[1] Ebrahimkhanlou, A., Athanasiou, A., Hrynyk, T. D., Bayrak, O., & Salamone, S. (2019). Fractal and Multifractal Analysis of Crack Patterns in Prestressed Concrete Girders. *Journal of Bridge Engineering*, *24*(7), 04019059.

[2] Suarez-Dominguez, Edgardo Palacio-Pérez, Arturo. Aranda-Jiménez, Yolanda & Izquierdo-Kulich, Elena. (2019). New Relation of Fluid Flow in Fractal Porous Medium: I. Theoretical Analysis. International Journal of Advanced Manufacturing Technology. 8. 2092-2099.

[3] Flores-Andrade, E., Pascual-Pineda, L. A., Quintanilla-Carvajal, M. X., Gutiérrez-López, G. F., Beristain, C. I., & Azuara, E. (2018). Fractal surface analysis and thermodynamic properties of moisture sorption of calcium–sucrose powders. *Drying technology*, *36*(9), 1128-1141.

[4] Wang, M., Chen, Y. F., Ma, G. W., Zhou, J. Q., & Zhou, C. B. (2016). Influence of surface roughness on nonlinear flow behaviors in 3D self-affine rough fractures: Lattice Boltzmann simulations. *Advances in water resources*, *96*, 373-388.

[5] Chen, Y., Wang, Y., & Li, X. (2019). Fractal dimensions derived from spatial allometric scaling of urban form. *Chaos, Solitons & Fractals*, *126*, 122-134.

[6] Abràmoff, M. D., Magalhães, P. J., & Ram, S. J. (2004). Image processing with ImageJ. *Biophotonics international*, *11*(7), 36-42.

[7] Sanchez-Medrano, T. & Suarez-Dominguez, E.J. (2019) Microscopic Analysis of Bamboo Pieces and Its Relation to Compression Resistance IJRTE. 8[3] 3809-3812.

[8] Edgardo J. Suarez-Dominguez, BenXu, Arturo Palacio-Perez et al. Stochastic modeling of asphaltenes deposition and prediction of its influence on friction pressure drop. *Petroleum Science and Technology*, 2018, vol. 36, no 21, p. 1812-1819.

